

## Response of Porcine Eyes to Blast Overpressure: Effects of Overpressure Severity and Boundary Conditions

A. R. Kemper<sup>1</sup>, V. D. Alphonse<sup>1</sup>, C. McNally<sup>1</sup>, I. P. Herring<sup>2</sup>, P. J. Brown<sup>1</sup>, J. D. Stitzel<sup>1</sup>, and S. M. Duma<sup>1</sup>

<sup>1</sup>Virginia Tech-Wake Forest University Center for Injury Biomechanics

<sup>2</sup>Virginia-Maryland Regional College of Veterinary Medicine

*This paper has not been screened for accuracy nor refereed by any body of scientific peers and should not be referenced in the open literature.*

### ABSTRACT

*Combat-related eye injuries are occurring more frequently with the increased use of explosive devices in current military conflicts. While numerous studies have shown that projectile impacts to the eye can cause serious damage to the eye and vision, little is known about the potentially injurious effects of the pressure wave associated with explosions. Therefore, current research focuses on isolating the pressure wave (i.e. primary blast) from other injury mechanisms to evaluate overpressure as a potential injury mechanism. The purpose of this study is to assess the response of the eye to overpressure using three boundary conditions of increasing biofidelity at three survivable overpressure levels. An Advanced Blast Simulator (ABS) was used to isolate and mimic overpressure profiles observed in combat. Pressure levels assessed were 10 psi, 20 psi, and 30 psi static overpressure, as measured along the inner wall of the ABS at the test site. Porcine eyes were tested in isolation, potted in a synthetic orbit, or potted in a 3D printed orbit, and exposed to a single overpressure event. Pressure was measured at various locations within the fluid flow, around the eye, inside the orbit, and inside the eye. Blast wave characteristics (i.e. peak overpressure, positive duration, and positive impulse) were calculated for each location at which pressure was measured. Peak intraocular pressure was used to calculate injury risk for physical and physiologic injuries using previously published injury risk functions. Dissection of each eye revealed that no macroscopic physical injuries were caused by overpressure exposure. In addition, the calculated injury risk for both physical and physiologic injuries due to overpressure exposure was extremely low at the severity levels evaluated in the current study. It is likely that the overpressure severity required to cause severe ocular injuries would likely result in other serious and potentially life-threatening injuries that would take precedence over potential eye injuries.*

*Data from these tests can be used to validate physical and finite element models of the eye and face for evaluating injury risk due to blast overpressure exposure.*

## INTRODUCTION

The increased use of explosives in current military conflicts has affected the epidemiology of combat-related injuries sustained by soldiers and civilians. The rate of eye injuries has dramatically increased in recent conflicts. Eye injuries accounted for approximately 2% of all injuries during World War I and World War II, and approximately 13% of all injuries during Operation Desert Storm (Wong et al., 2000, Heier et al., 1993,). Given the increased development and more widely accepted use of ballistic personal protective equipment, injuries that were once fatal are now survivable. Injuries to the eye, which were at one time ignored due to their low threat to life, now pose a larger problem as they can affect the ability of soldiers to meet return-to-duty standards following injury.

A blast event comprises four potentially injurious mechanisms; primary, secondary, tertiary, and quaternary. Primary blast injuries are caused solely by the pressure wave that precedes any fragmentation or debris. Secondary blast injuries are caused by projected material, and are often penetrating or perforating wounds. Tertiary blast injuries are caused by impacting other objects, such as walls and floors, when the body is propelled by the event. Quaternary blast injuries include all other injuries related to blasts, including thermal and radiation burns, exposure to chemicals, and miscellaneous injuries. It was previously determined that between 68% and 78% of eye injuries are caused by blast fragments (Cimberle, 2007) and that 80% of severe injuries are due to blast fragmentation (Mader et al., 2006). Personal protective eye equipment such as glasses and goggles are currently only tested for ballistic situations. Although glasses and goggles can prevent many cases of secondary blast injuries to the eye, there is a lack of consistent use recorded with documented eye injuries. As much as 85% of reported ocular injuries are associated with either protective eyewear non-compliance or unknown eyewear status at the time of injury (Thach et al., 2005). Another study showed that only 26% of those injured wore protective eyewear at the time of injury (Mader et al., 2006). Numerous studies have been performed to evaluate the response and injury tolerance of the eye due to projectile impacts (Weidenthal and Schepens, 1966, Delori et al., 1969, Vinger et al., 1999, Stitzel et al., 2002, Kennedy et al., 2006, Kennedy et al., 2007, Duma et al., 2012). Ultimately, injury data from these studies have been used to validate physical and finite element models of the eye and to develop risk functions for projectile impacts to the eye.

While secondary, tertiary, and quaternary injury mechanisms are well understood, specific injury mechanisms unique to primary blast are largely hypothetical. Numerous authors have reported that mild to severe eye injuries, including hyphema, conjunctival hemorrhage, retinal edema, retinal detachments, globe rupture, and orbital fracture, can be caused by primary blast (Mayorga, 1997, DePalma et al., 2005, Ritenour and Baskin, 2008, Wolf et al., 2009). However, there is a paucity of empirical evidence in the literature to support this. One study previously evaluated the response of the human eye to overpressure; however, this focused on low-level overpressure (less than 5 psi, static overpressure), reported no injuries caused by overpressure, and was performed on isolated eyes (Alphonse et al., 2012). Consequently, it remains unclear how primary blast overpressure may affect the eye. Therefore, the purpose of the current research is to examine primary blast injuries related to the unprotected eye. Specifically, this work aims to evaluate exposure to higher energy pressure waves as a potential eye injury mechanism, and to quantify the effect of reflected surfaces surrounding the eye.

## METHODS

The small Virginia Tech Advanced Blast Simulator (ABS) was used to simulate blast overpressures. The cross-sectional area of the test region is 1ft by 1ft, and was designed for testing small objects (Figure 1). The driver and driven sections of the ABS were separated by a membrane. The driver section was rapidly filled with helium until the membrane passively ruptured, generating an overpressure wave which traveled down the ABS to the test region. Aluminum membranes were used to create an isolated overpressure wave with no fragmentation. Various aluminum alloys and plate thicknesses were used to reach static overpressure

levels of 10 psi, 20 psi, and 30 psi within 3 psi as measured along the wall of the ABS at the test region. A CNC mill was used to consistently score an “X” pattern on each membrane. This scoring pattern facilitated a near-instantaneous rupture of the membrane and did not produce fragments.

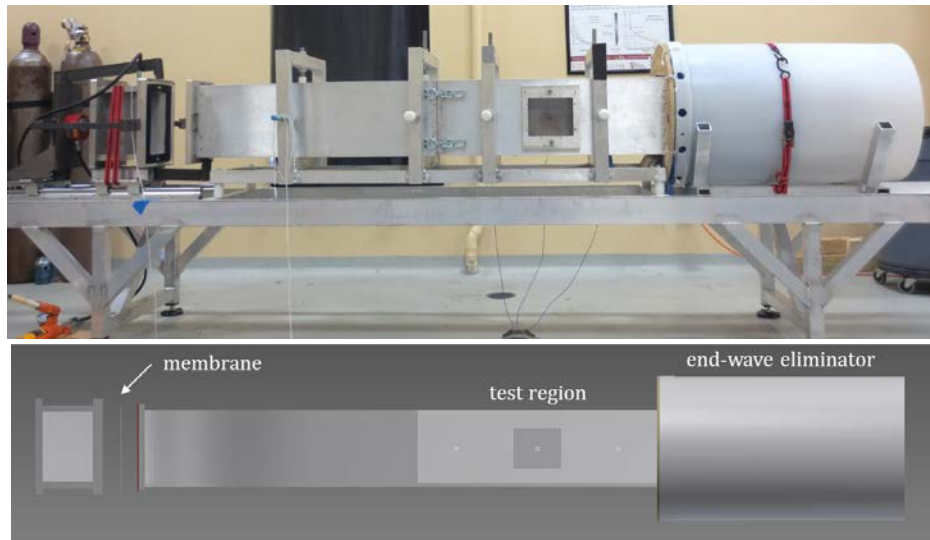
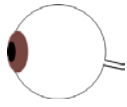
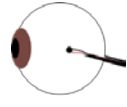
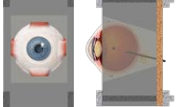


Figure 1: Advanced Blast Simulator at Virginia Tech.

### Test Matrix and Boundary Conditions

The proposed porcine eye test matrix includes 45 overpressure tests using three boundary conditions and three overpressure severities, as well as five control eyes and five sham eyes (Table 1). Currently, 27 of the tested eyes are completed. Three boundary conditions surrounding the eye, described below, were tested to evaluate the effect of reflective surfaces around the eye. Fresh porcine eyes with long optic nerves were shipped overnight on wet ice from Animal Technologies (Tyler, TX) and tested within three days of death. Any skin and muscle surrounding the globe was carefully removed. Eyes that were used for controls were dissected at this point to assess postmortem and procurement damage. Sham and test eyes were further prepared by applying a dot pattern on the sclera using permanent black ink. A small tube and a miniature pressure sensor were inserted into the vitreous fluid through the optic nerve and secured in place. Sham eyes were pressurized to physiologic intraocular pressure and dissected to assess damage caused by these preparation methods. Test eyes were then potted in one of the three boundary conditions (Figure 2).

Table 1. Proposed porcine eye test matrix for the testing described herein. Altogether, 55 tests are planned; 45 of these tests will be exposed to blast overpressure. Currently, 27 of the tested eyes are completed.

Porcine Eye Test Matrix				
Control	Sham	Isolated Eye	Synthetic Orbit	3D Orbit
				
5 eyes (no blast)	5 eyes (no blast)	15 eyes (5 at each pressure level)	15 eyes (5 at each pressure level)	15 eyes (5 at each pressure level)
Quantify baseline conditions for postmortem, procurement, and dissection damage	Quantify damage from preparation methods (pressurization tube and pressure sensor)	Quantify pressure wave propagation through eye	Quantify IOP and reflected pressure on the forehead, and within the orbit with gelatin around eye	Quantify IOP and reflected pressure around the face and within the orbit with gelatin around the eye

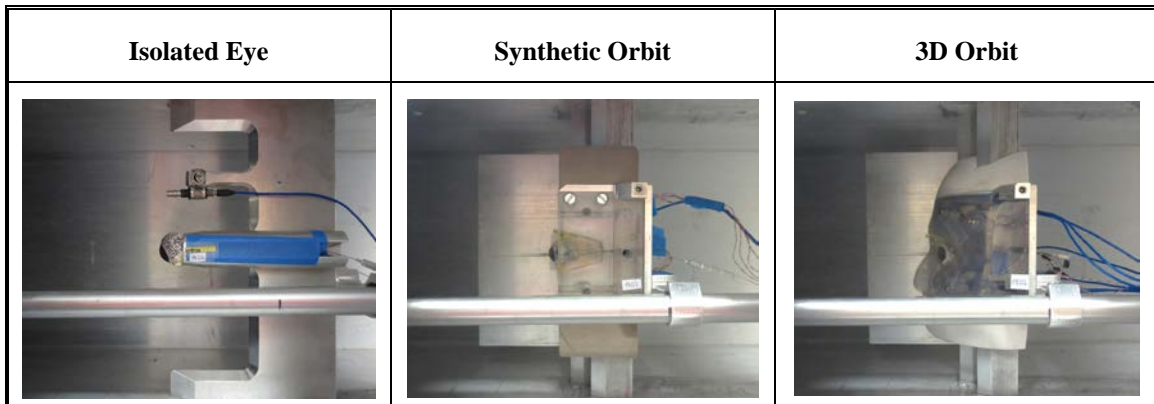


Figure 2. Photographs of each test setup: isolated eye (left), synthetic orbit (middle), and 3D orbit (right). Note: The pencil sensor that measures static overpressure within the flow is shown in the forefront of each image. The sensing element on the pencil sensor is flush with the cornea of the eye.

*Isolated Eye.* The isolated eye condition examined the effects of overpressure on an isolated, unobstructed eye. This served as a baseline condition for understanding the pressure wave propagation within the eye, and did not represent a physical analog of a real-life event. Once prepped with the pressurization tube and miniature pressure sensor, the eye was placed in a custom holder that consisted of a rigid concave aluminum cup. The optic nerve was threaded through a hole in the back of the cup and secured in place. A small shelf at the bottom of the cup allowed the eye to rest in a neutral, forward-facing position. The eye was minimally constricted by this placement, and equatorial expansion was not limited by contact with the cup. A pressure sensor located above the isolated eye approximately where the forehead would be measured the total overpressure of the fluid flow. Static overpressure along the wall and in the fluid flow, total overpressure in the fluid flow, and intraocular overpressure were recorded for all isolated tests.

*Eye in Synthetic Orbit.* The synthetic orbit condition examined the effects of overpressure on a simple orbital geometry with the gelatin that simulated the orbital fat and musculature surrounding the eye. This condition can be easily reproduced in a finite element model for validation. The synthetic orbit was made of simple, flat surfaces that provided a first order approximation of the geometry of the human orbit. Once prepped with the pressurization tube and miniature pressure sensor, the eye was placed in the orbit and surrounded by a 10% Knox® solution. One pressure sensor was placed flush with the front-facing surface above the eye, and measured reflected pressure at the forehead. Additionally, four pressure sensors located within the orbit measured how the pressure wave propagated through the gelatin and around the eye in the frustum-shaped orbit. Three sensors were placed 0.5" from the front surface; one was placed on the maxillary bone, one was placed on the lacrimal/ethmoid bone, and one placed on the frontal bone. In addition, one sensor was placed on the frontal bone 1" from the front surface. Static overpressure along the wall and in the fluid flow, reflected overpressure at the forehead, four intraorbital overpressures, and intraocular overpressure were recorded for all synthetic orbit tests. A plane of symmetry along the nasal side of the orbit was used to recreate a more realistic fluid flow.

*Eye in 3D Printed Orbit.* The 3D orbit condition examined the effects of overpressure on a complex orbital and facial geometry, and served as the most biofidelic of the three test conditions. The 3D printed orbit was made from the facial geometry, including the skin, of the Global Human Bodies Model Consortium (GHBMC). Once prepped with the pressurization tube and miniature pressure sensor, the eye was placed in the orbit and surrounded by a 10% Knox® solution. Four pressure sensors were placed within the orbit, as described above for the synthetic orbit. Additionally, seven pressure sensors were placed flush with the skin around the face; one near the tear duct, three along the forehead, and three along the chin (Figure 3). Static overpressure along the wall and in the fluid flow, reflected overpressure around the face, four intraorbital overpressures, and intraocular overpressure were recorded for all 3D orbit tests (same locations as those used in the synthetic orbit). A plane of symmetry along the nasal side of the orbit was used to recreate a more realistic fluid flow.

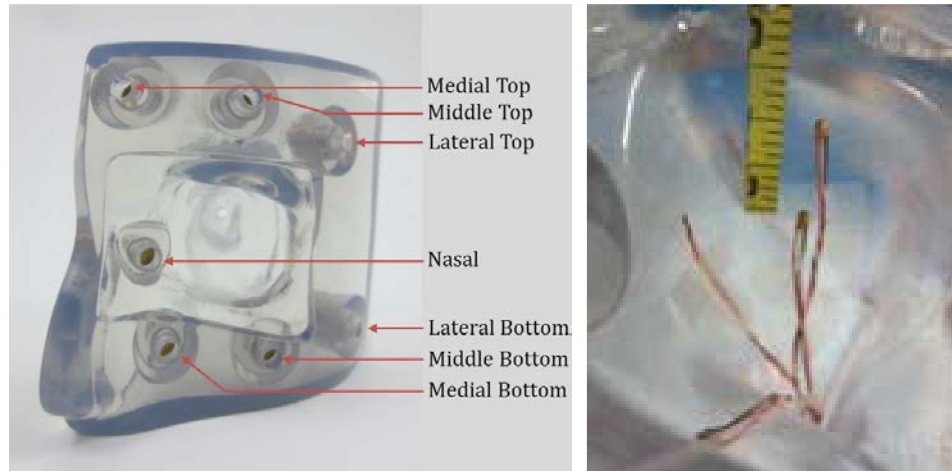


Figure 3. Pressure sensor locations around (left) and within (right) the 3D orbit. Note that all extraorbital sensors are flush with the “skin” surface of the orbit.

## Instrumentation

All pressure data were collected at 300 kHz using TDAS Pro (DTS TDAS PRO, Seal Beach, CA). High speed video of each event was recorded at 10 kfps (Phantom v9.1, Vision Research, Wayne, NJ). Miniature pressure sensors were used to measure intraocular and intraorbital overpressures (Model 060, 060s, Precision Measurement Company, Ann Arbor, MI). Static overpressure was measured along the wall of the tube in three locations that were 12” apart, with the middle sensor at the test region (Model 102B16, PCB Piezotronics). Static overpressure within the flow was measured with a pencil sensor (Model 137A24, PCB Piezotronics). Reflected overpressure was measured along the surfaces of the synthetic and 3D orbits (Model 113B21, PCB Piezotronics). Total overpressure was measured above the isolated eye (Model 113B21, PCB Piezotronics). All PCB Piezotronics sensors were designed specifically for use with blast loading conditions.

## Analyses

*Blast Wave Characteristics.* All pressure data were zeroed prior to the blast event. Peak overpressure, positive duration, and positive impulse were calculated from each overpressure trace for each measurement location. Peak overpressure was defined as the maximum pressure recorded during a test. Infrequently, extremely short duration spikes in the pressure trace caused by instrumentation vibration were excluded from peak overpressure determination. Positive duration was defined as the time interval between initiation of positive overpressure and the time at which the pressure returns to zero. Positive impulse was calculated using trapezoidal integration of the pressure trace over the positive duration. Impulse was influenced by both peak overpressure and positive duration. Peak overpressure, positive duration, and positive impulse were compared for all pressure measurement locations. Peak intraocular overpressure was correlated to both static overpressure and total or reflected overpressure at the forehead.

*Injury Assessment.* Each eye was examined prior to and following exposure to the overpressure event for macroscopic injury and displacement of structures. Corneal damage caused by postmortem effects, procurement techniques and preparation was assessed by applying fluorescein dye to the cornea and visualizing any abrasions with the use of a blue light. Following the test, this was repeated to quantify any changes due to overpressure exposure. The cornea was then removed to expose the iris and anterior portion of the lens. Any gross injuries to the iris or anterior portion of the lens were noted. The iris was carefully cut away to expose the underlying ciliary body and zonules. A trinocular surgical microscope was used to examine the zonules; a small amount of tension was placed on the lens and the contralateral portion of the iris to observe any damaged zonules. Finally, the eye was bisected equatorially to expose the posterior portion of the lens and ciliary body, as well as the retinal surfaces. These structures were examined for gross damage. Due to rapid postmortem degradation, retinal damage was not positively correlated to exposure to blast overpressure; retinal damage was present in all eyes, including those that were used as controls and shams.

*Injury Risk Determination.* Peak intraocular overpressure was used to quantify injury risk for hyphema, lens damage, retinal damage, and globe rupture. Specifically, normalized energy was calculated using the equation for a 11.16 mm diameter rod, as the area of this projectile most closely resembles the area of the unprotected eye that would be exposed to blast overpressure (Duma et al, 2012). Normalized energy was then correlated to injury risk using previously published injury risk curves (Duma and Kennedy, 2012).

## RESULTS

Peak overpressure increased for all pressure measurement locations with increasing pressure level (Figure 4). Static overpressure was relatively consistent for all orbits. Reflected overpressure was highest for the synthetic orbit for all severity levels. Intraocular overpressure was highest for the synthetic orbit at the 10 psi and 20 psi levels; intraocular pressure was highest for the 3D orbit at the 30 psi level. Peak intraocular overpressure was correlated to peak static overpressure and peak reflected overpressure for all boundary conditions using data from all pressure levels. Peak intraocular overpressure was best correlated to peak reflected overpressure for all boundary conditions.

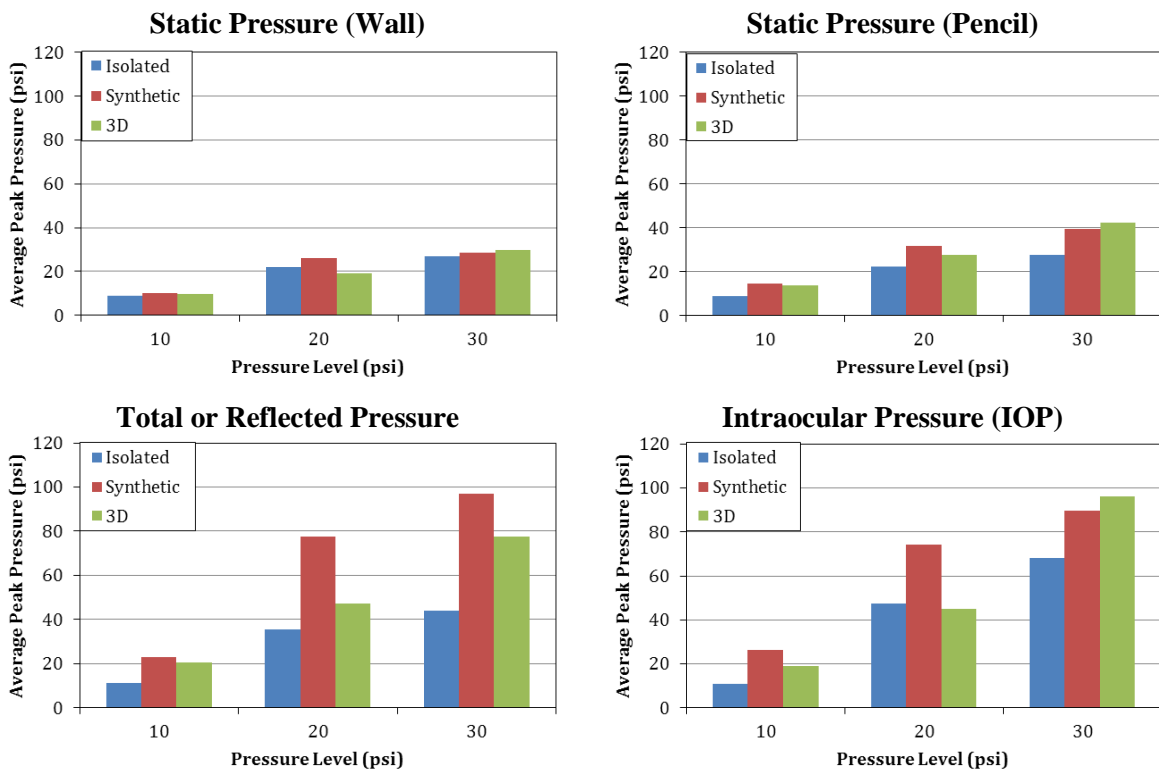


Figure 4. Average peak overpressure for static overpressure measured at the wall (top, left), static overpressure measured in the flow (top, right), reflected/total overpressure (bottom, left), and intraocular overpressure (bottom, right). Note: The total overpressure pressure sensor used in the isolated condition was compared to the reflected pressure sensors used in the synthetic and 3D orbits.

Overpressure traces for intraocular overpressure, static overpressure (“pencil”), and reflected overpressure are shown for the 20 psi tests for each boundary condition in Figure 5. Note that the intraocular overpressure traces more closely resemble the reflected overpressure traces than the static overpressure traces. This is due to the fact that the forward-facing eye and forehead sensors will record both the static and dynamic components of the overpressure wave because they are perpendicular to the pressure wave propagation. Also note the consistent response at each sensor location.

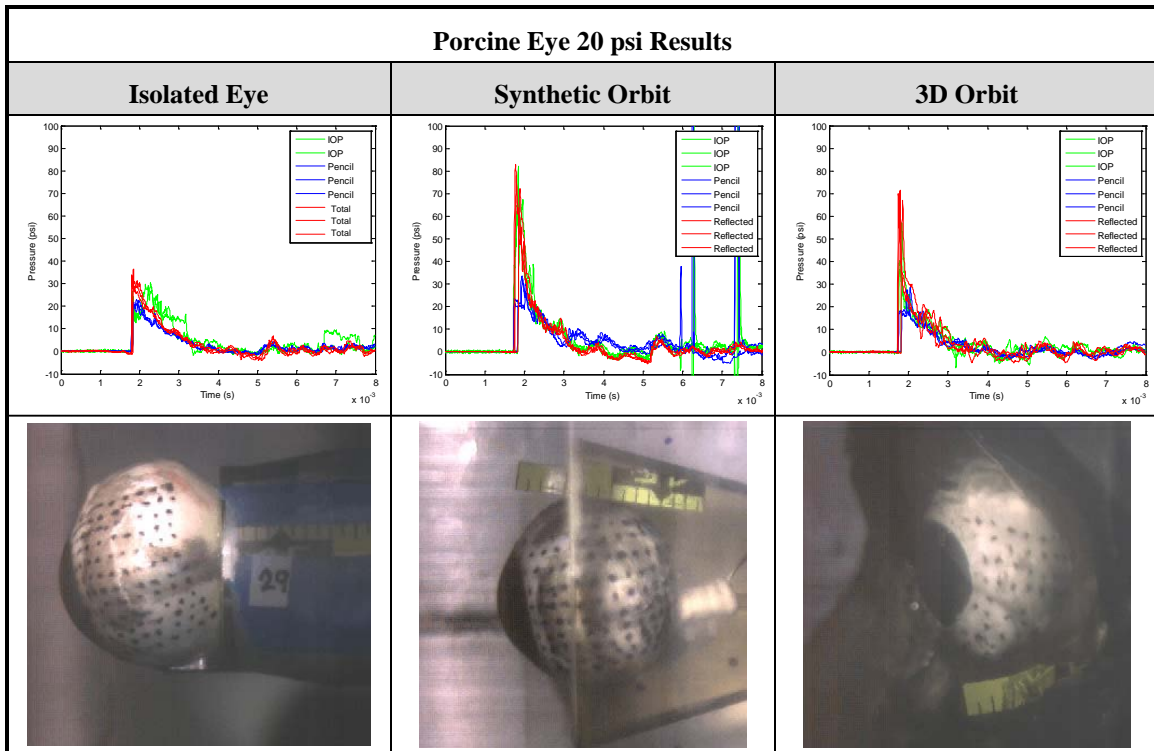


Figure 5. Overpressure traces for the three boundary conditions, showing intraocular overpressure, static overpressure, and reflected overpressure. Still images from high speed video show the position of the eye within each boundary condition.

The temporal responses for each of the reflected overpressure sensors on the face of the 3D orbit are shown in Figure 6. The peak overpressure and initiation of positive overpressure (i.e. initial pick up) varied by with respect to sensor location. Most notably, the sensors located on the lateral portion of the face recorded lower peak overpressures and had delayed overpressure onset times as compared to those located on the medial portion of the face.

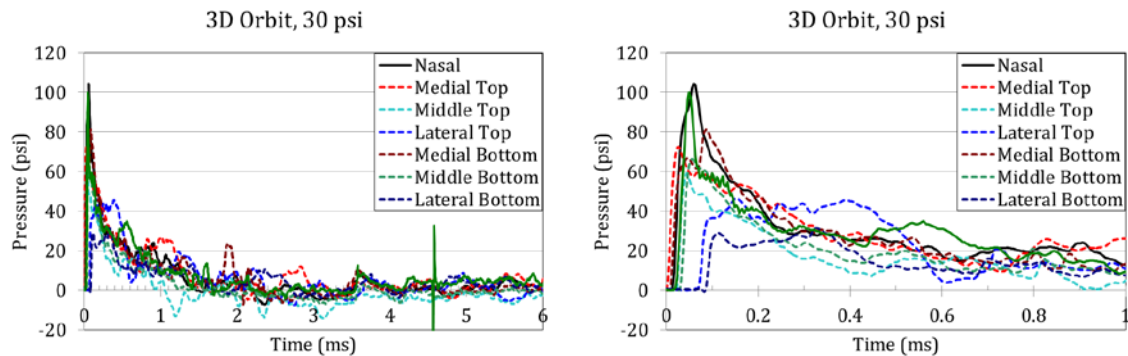


Figure 6. Reflected overpressure traces for the facial locations on the 3D orbit for a 30 psi test. Note the temporal pickup for each location is related to the distance to the pressure wave. All pressure traces are zeroed based on the Nasal location.

Dissection of each eye resulted in no macroscopic damage caused by exposure to blast overpressure. The photographs in Figure 7 show typical images collected during dissection. The eye shown in these photographs was potted in the synthetic orbit and exposed to a single 30 psi event. The deterioration of the posterior retina, as seen in Figure 7e, was observed in control and sham eyes as well as those that were tested.

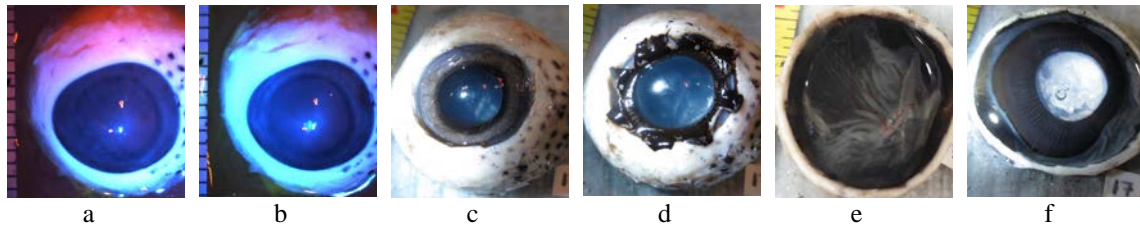


Figure 7. Fluorescein dye applied to the cornea to assess corneal abrasion, (a) pre-test, (b) post-test. Cornea removed to expose the anterior portion of the ciliary body and iris (c). Iris removed to expose zonules and lens (d). Eye bisected to expose posterior retina (e) and the posterior portion of the ciliary body and lens (f).

The ink dots and anatomical locations on the eye were tracked manually using high-speed video. Figure 8 shows the synthetic orbit condition at 10 psi, 20 psi, and 30 psi for 30 frames, which corresponded to the first 3 ms of each test. The resolution of the video stills was at least 5 pixels per millimeter. There was minimal corneal deflection and globe translation in some of the tests at the higher pressure levels, though anterior-posterior movement was less than 3 mm.

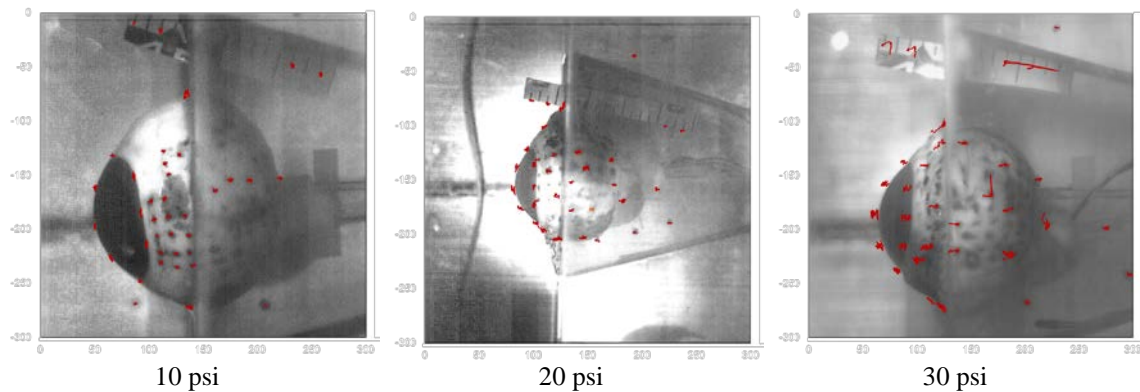


Figure 8. Still images from high-speed video. Red lines show the tracking of anatomical locations and ink dots on the sclera for 30 frames (3 ms). All images are for the synthetic orbit.

Injury risk for hyphema, lens damage, retinal damage, and globe rupture was calculated using peak intraocular overpressure for each test. The average injury risk for lens damage, retinal damage, and globe rupture was less than or equal to 0.02% for each boundary condition and severity level. The average injury risk for hyphema was less than or equal to 2% for each boundary condition and severity level.

## CONCLUSIONS

Twenty-seven porcine eyes potted in one of three boundary conditions (isolated eye, synthetic orbit, or 3D orbit) were exposed to a single static overpressure event at 10 psi, 20 psi, or 30 psi (static overpressure) using an Advanced Blast Simulator. Results show trends in peak overpressure with respect to both pressure level and boundary condition. Naturally, all peak overpressures increased with increasing pressure level. Intraocular pressure was most highly correlated to forehead reflected pressure for the synthetic and 3D orbits. Intuitively, both the eye and forehead were expected to experience the greatest overpressures due to their forward-facing direction with respect to the blast wave propagation. The flat surfaces of the synthetic orbit were most restrictive to fluid flow, and therefore resulted in the highest reflected pressures at the forehead of the three boundary conditions. Reflected overpressures measured on the face of the 3D orbit showed that the peak overpressure and initiation of positive overpressure (i.e. initial pick up) varied by with respect to sensor location. The data from these sensors can be used to further validate the response of complex computational models of the face and eye during blast overpressure events.

No injuries were caused by overpressure exposure. In addition, the calculated injury risk for all injuries assessed was extremely low (< 2%) for all pressure levels and boundary conditions. These results are consistent with the lack of injuries observed and reported in theatre caused solely by overpressure. It should be noted that although the overpressure levels studied herein are higher than those previously examined, the overpressure waves produced by the ABS in the current study are at the threshold of lung injury and are likely survivable (Stuhmiller et al., 1995). Therefore, it is hypothesized that the overpressure levels needed to cause gross eye injury will likely cause other more serious injuries to other regions of the body.

Once completed, this research will provide novel data for the validation of physical and finite element models used to assess blast-induced injury risk to the eye. This data will improve the understanding of pressure wave propagation through and around the orbit. Future work using an anesthetized animal model will expand upon the data presented currently, as functional and physiological injuries could not be assessed with the current enucleated post-mortem eye model. Additionally, although porcine eyes are anatomically similar to human eyes, evaluating human eyes in the three boundary conditions will yield more realistic injury results for human injury risk assessment. Comparisons between porcine and human eye response would be beneficial for future research.

## ACKNOWLEDGEMENTS

The authors would like to acknowledge the United States Army Medical Research and Materiel Command for their support of this research and development program, Dr. Pamela J. VandeVord for providing the Advanced Blast Simulator, Dr. Joel D. Stitzel and Philip J. Brown for printing the 3D orbit, Dr. Ian P. Herring for ophthalmic consultation, Craig McNally for manufacturing parts and membranes, and Anna M. MacAlister and Stephanie M. Beeman for their assistance throughout this test series.

## REFERENCES

- ALPHONSE, V. D., KEMPER, A. R., STROM III, B. T., BEEMAN, S. M., and DUMA, S. M. Mechanisms of eye injuries from fireworks. (2012). *JAMA*, 308(1):33-34.
- CIMBERLE, M. Wartime incidence of eye injuries surging, medical officer says. (2007) *Ocular Surgery News*, 25(2):102-103.
- DELORI, F., POMERANTZEFF, O., and COX, M. S. Deformation of the globe under high-speed impact: Its relation to contusion injuries. (1969). *Invest Ophthalmol*, 8(3):290-301.
- DEPALMA, R. G., BURRIS, D. G., CHAMPION, H. R., and HODGSON, M. J. (2005). Blast injuries. *N Engl J Med*, 352(13):1335-1342.
- DUMA, S. M., BISPLINGHOFF, J. A., SENGE, D. M., MCNALLY, C., and ALPHONSE, V. D. (2012a). Evaluating the risk of eye injuries: Intraocular pressure during high speed projectile impacts. *Curr Eye Res*, 37(1):43-49.
- DUMA, S. M., KENNEDY, E. A. (2012b), Final report: eye injury risk functions for human and FOCUS eyes: hyphema, lens dislocation, and retinal damage. <[http://www.facstaff.bucknell.edu/eak012/Reports\\_n\\_Papers/Eye\\_Injury\\_Risk\\_Functions\\_for\\_Human\\_and\\_FOCUS\\_Eyes--FinalReport\\_W81XWH-05-2-0055--July2011Update.pdf](http://www.facstaff.bucknell.edu/eak012/Reports_n_Papers/Eye_Injury_Risk_Functions_for_Human_and_FOCUS_Eyes--FinalReport_W81XWH-05-2-0055--July2011Update.pdf)>. Accessed May 29, 2012.
- HEIER, J. S., ENZENAURER, R. W., WINTERMEYER, S. F., DELANEY, M., and LAPIANA, F. P. (1993). Ocular injuries and diseases at a combat support hospital in support of Operations Desert Shield and Desert Storm. *Arch Ophthalmol*, 111(6):795-798.

- KENNEDY, E. A., NG, T. P., MCNALLY, C., STITZEL, J. D., and DUMA, S. M. Risk functions for human and porcine eye rupture based on projectile characteristics of blunt objects. (2006). *Stapp Car Crash J*, 50:651-671.
- KENNEDY, E. A., INZANA, J. A., MCNALLY, C., and DUMA, S. M. Development and validation of a synthetic eye and orbit for estimating the potential for globe rupture due to specific impact conditions. (2007). *Stapp Car Crash J*, 51:381-400.
- MADER, T. H., CARROLL, R. D., SLADE, C. S., GEORGE, R. K., RITCHEY, P., and NEVILLE, S. P. (2006). Ocular war injuries of the Iraqi Insurgency, January-September 2004. *Ophthalmology*, 113(1):97-104.
- MAYORGA, M. A. The pathology of primary blast overpressure injury. (1997). *Toxicology*, 121(1):17-28.
- RITENOUR, A. E., and BASKIN, T. W. (2008) Primary blast injury: Update on diagnosis and treatment. *Crit Care Med*, 36(7 Suppl):S311-S317.
- STITZEL, J. D., DUMA, S. M., CORMIER, J. M., and HERRING, I. P. (2002). A nonlinear finite element model of the eye with experimental validation for the prediction of globe rupture. *Stapp Car Crash J*, 46:81-102.
- STUHMILLER, J. H., HO, K. H.H., VANDER VORST, M. J., DODD, K. T., FITZPATRICK, T., and MAYORGA, M. (1995). A model of blast overpressure injury to the lung. *J Biomech*, 29(2):227-234.
- THACH, A. B., JOHNSON, A. J., CARROLL, R. B., HUCHUN, A., AINBINDER, D. J., STUTZMAN, R. D., BLAYDON, S. M., DEMARTELAERE, S. L., MADER, T. H., SLADE, C. S., GEORGE, R. K., RITCHEY, J. P., BARNES, S. D., and FANNIN, L. A. (2007). Severe eye injuries in the War in Iraq, 2003-2005. *Ophthalmology*, 115(2):377-382.
- VINGER, P. F., DUMA, S. M., and CRANDALL, J. (1999). Baseball hardness as a risk factor for eye injuries. *Arch Ophthalmol*, 117:354-358.
- WEIDENTHAL, D. T., and SCHEPENS, C. L. (1966). Peripheral fundus changes associated with ocular contusion. *Am J Ophthalmol*, 62(3):465-477.
- WOLF, S. J., BEBARTA, V. S., BONNETT, C. J, PONS, P. T., and CANTRILL, S. V. (2009). Blast injuries. *Lancet*, 374(9687):405-415.
- WONG, T. Y., SMITH, G. S., LINCOLN, A. E., and TIELSCH, J. M. (2000). Ocular trauma in the United States Army: Hospitalization records from 1985 through 1994. *Am J Ophthalmol*, 129(5):645-650.